Stochastic forcing of the linearized Navier–Stokes equations

Brian F. Farrell
Department of Earth and Planetary Sciences, Harvard University, Cambridge, Massachusetts 01238

Petros J. Ioannou
Center for Meteorology and Physical Oceanography, Massachusetts Institute of Technology, Cambridge, Massachusetts 02138

(Received 16 September 1992; accepted 13 July 1993)

Transient amplification of a particular set of favorably configured forcing functions in the stochastically driven Navier–Stokes equations linearized about a mean shear flow is shown to produce high levels of variance concentrated in a distinct set of response functions. The dominant forcing functions are found as solutions of a Lyapunov equation and the response functions are found as the distinct solutions of a related Lyapunov equation. Neither the forcing nor the response functions can be identified with the normal modes of the linearized dynamical operator. High variance levels are sustained in these systems under stochastic forcing, largely by transfer of energy from the mean flow to the perturbation field, despite the exponential stability of all normal modes of the system. From the perspective of modal analysis the explanation for this amplification of variance can be traced to the non-normality of the linearized dynamical operator. The great amplification of perturbation variance found for Couette and Poiseuille flow implies a mechanism for producing and sustaining high levels of variance in shear flows from relatively small intrinsic or extrinsic forcing disturbances.

I. INTRODUCTION

Transition to turbulence typically occurs in channel flow experiments at $R=O(1000)$, where R is the flow Reynolds number based on the mean centerline velocity and the half-width of the channel. Careful control of the intensity of disturbances results in persistence of laminar flow to much higher Reynolds numbers, which for pipe Poiseuille flow[1,2] can reach as high as $R\approx 50\,000$. The dynamics of such small perturbations as are associated with high R transition can, at least initially, be described with accuracy by the Navier–Stokes equations linearized about the background flow. Assuming that disturbances of whatever origin can be modeled as noise, it is of interest to address, making use of linearized perturbation theory, the level of variance sustained in the mean by stochastic forcing. Moreover, it is well known[3] that even in fully turbulent flows the linear growth mechanism is solely responsible for the transfer of energy from the mean flow to perturbations, so that a complete characterization of this linear mechanism is a necessary step toward understanding turbulent flows.

The familiar problem of the damped harmonic oscillator excited by random and uncorrelated impulses exemplifies the physical processes operating in the most familiar dynamical systems. It can be shown that the ensemble average variance of the displacement, x, of the oscillator is given by

$$\langle |x|^2 \rangle = \frac{\dot{\epsilon}}{2\gamma\omega^2}, \tag{1}$$

where $\dot{\epsilon}$ is the variance of the random forcing, ω is the natural frequency of the oscillator, and γ is the damping coefficient.[4] When $\omega=0$ there is no restoring force, and we obtain Brownian motion, which is not stationary. When $\gamma=0$ there is no damping, and random driving again leads to nonstationary statistics, while for nonvanishing restoring force and nonvanishing damping the variance reaches a finite statistically stationary level, such that the input of energy from the driving balances the dissipation, and the variance level is inversely proportional to the damping coefficient. This behavior is characteristic of all dynamical systems with normal dynamical operators. The total variance in such systems is the sum of the variance of each of the normal modes taken separately, the same as if each mode were independently excited by stochastic forcing.

Consider now a fluid with a background flow field having nonvanishing rate of strain, but with sufficient dissipation so that all small perturbations impressed on the flow eventually decay. Linearization of this dynamical system about its background flow results in a non-normal dynamical operator and an associated set of modes that are not mutually orthogonal, either in the inner product associated with the L_2 or the energy norm. This lack of orthogonality corresponds to the potential for extraction of energy by the perturbations from the background flow, irrespectively of the existence of exponential instabilities, a result well known since the seminal work of Orr.[5] The energy balance in such a system is between the stochastic forcing, together with the induced extraction of energy from the background flow, on the one hand, and the dissipation on the other. Without stochastic forcing the perturbation field would vanish. With stochastic forcing an enhanced level of variance can be maintained by the stochastically induced transfer of background flow energy to the perturbation field, and this level of variance may exceed that arising simply by accumulation of energy from the forcing. In this respect stochastically forced non-normal dynamical systems differ fundamentally from the classical problem of stochastically forced coupled harmonic oscillators.

 0899-8213/93/5(11)/2600/10/$6.00

These considerations led Farrell and Ioannou[6] to investigate the variance maintained by stochastic forcing in two-dimensional (2-D) unbounded constant shear and deformation flows. It was found that the variance in pure deformation flows increases without bound under stochastic excitation for any value of the viscosity. In contrast, in shear flow the variance was found to be limited to an increase of a factor of 3 over that arising from the same forcing of the unsheared fluid, which is governed by a normal dynamical operator.

Interest in studying stochastic forcing of 3-D perturbations in channel flows was motivated by the calculations of Butler and Farrell,[7] Farrell and Ioannov,[8] Gustavsson,[9] and Reddy and Henningson,[10] in which it was found that the maximal growth of 3-D perturbations in channel flows far exceeds the growth of their 2-D counterparts, and is simultaneously more persistent. This great amplification found for a subset of 3-D perturbations in shear flow strongly suggests, but does not prove that stochastic forcing of 3-D perturbations in shear flow induces much higher variance levels than were found in the above study of stochastically forced 2-D perturbations in unbounded constant shear flow. In this work it is demonstrated that the potential for greatly enhanced variance in shear flows subjected to 3-D stochastic forcing is realized and crucially depends on the non-normality of the underlying dynamical operator. While unbounded constant shear flow has the convenient property, exploited in the aforementioned works, of a closed form solution, this is not true for bounded flows, so in this work a general method is presented that is valid, in principle, for calculating the response of any bounded flow to stochastic forcing.

II. STOCHASTIC FORCING OF LINEAR NON-NORMAL DYNAMICAL SYSTEMS

Consider the linear autonomous dynamical system:

$$\frac{d}{dt}x_i=\mathscr{A}_{ij}x_j+\mathscr{F}_{ij}\xi_j. \tag{2}$$

The linear dynamical operator, $\mathscr{A}$, which controls the deterministic evolution of the system is, in general, non-normal [i.e., $\mathscr{A}^\dagger\mathscr{A}\neq\mathscr{A}\mathscr{A}^\dagger$, where $(\dagger)$ denotes the Hermitian transpose]. The stochastic nature of the dynamical system stems from the random nature of the forcing, ξ. This forcing is assumed to be a δ-correlated Gaussian white-noise process with zero mean:

$$\begin{aligned}&\langle\xi_i\rangle=0,\\&\langle\xi_i(t)\xi_j^*(t')\rangle=\dot{\epsilon}_i\delta_{ij}\delta(t-t'),\end{aligned} \tag{3}$$

where $\langle\ \rangle$ denotes ensemble averaging, and the asterisk denotes complex conjugation. This random forcing specification excites independently each forcing function, specified by the columns $f^{(j)}$ of the matrix $\mathscr{F}_{ij}$. Unless otherwise indicated all $\dot{\epsilon}_i$ will be taken of equal magnitude $\dot{\epsilon}$, which due to the linearity of the dynamical equation can be set equal to unity without any loss of generality. We want to determine the evolution of the variance sustained by (2), in which generalized velocities have been chosen in a manner to be described in the sequel, such that the ensemble average energy density is given by $\langle E^t\rangle=\langle x_i^*(t)x_i(t)\rangle$. When the dynamical system approaches a statistically steady state, the ensemble average energy density of this statistically steady state is given by $\langle E^\infty\rangle=\lim_{t\to\infty}\langle x_i^*(t)x_i(t)\rangle$.

The solution of (2) for $t\geqslant 0$, with initial condition x_0 is given by

$$x(t)=e^{\mathscr{A}t}x_0+\int_0^t\mathscr{G}(t-s)\mathscr{F}\xi\,ds, \tag{4}$$

where $\mathscr{G}(t-s)\equiv e^{\mathscr{A}(t-s)}$ is the Green's function. The random response, x, is linearly dependent on ξ and consequently is also Gaussian distributed. The statistics of the response of the dynamical system are consequently fully characterized by the first two moments.

The first moment, the average value of the generalized velocities, is given by $\langle x\rangle=e^{\mathscr{A}t}x_0$ and vanishes for large times if all the eigenvalues of $\mathscr{A}$ have negative real part, i.e., if $\mathscr{A}$ is asymptotically stable, leading to statistics that are independent of the initial conditions. In the sequel, we will consider only the inhomogeneous solution of (4), anticipating that at large times the asymptotic stability of $\mathscr{A}$ will render the statistics independent of the initial conditions.

The second moment, the ensemble average energy density, can be obtained making use of the assumed statistics of the forcing (3) as

$$\begin{aligned}\langle E^t\rangle&=\langle x_i^*(t)x_i(t)\rangle\\&=\int_0^t ds\int_0^t ds'\ \mathscr{G}_{ia}^*(t-s)\mathscr{F}_{ab}^*\langle\xi_b^*(s)\xi_d(s')\rangle\\&\quad\times\mathscr{G}_{ic}(t-s')\mathscr{F}_{cd}\\&=\mathscr{F}_{ba}^\dagger\left(\int_0^t\mathscr{G}_{ai}^\dagger(t-s)\mathscr{G}_{ic}(t-s)ds\right)\mathscr{F}_{cb}\\&=\sum_b f_a^{\dagger(b)}\mathscr{B}_{ac}^t f_c^{(b)}.\end{aligned} \tag{5}$$

We have defined

$$\mathscr{B}^t\equiv\int_0^t\mathscr{G}^\dagger(t-s)\mathscr{G}(t-s)ds=\int_0^t e^{\mathscr{A}^\dagger(t-s)}e^{\mathscr{A}(t-s)}\,ds, \tag{6}$$

and $f_a^{(b)}\equiv\mathscr{F}_{ab}$. Recall that $f_a^{(b)}$ represents the ath coordinate of the bth forcing function.

Setting $\tau=t-s$ in (6), we have $\mathscr{B}^t=\int_0^t e^{\mathscr{A}^\dagger\tau}e^{\mathscr{A}\tau}\,d\tau$, and differentiating with respect to time, we obtain

$$\frac{d}{dt}\mathscr{B}^t=e^{\mathscr{A}^\dagger t}e^{\mathscr{A}t}. \tag{7}$$

When $\mathscr{A}$ is asymptotically stable, we have from (7) that

$$\lim_{t\to\infty}\frac{d}{dt}\mathscr{B}^t=0. \tag{8}$$

The vanishing of $(d/dt)\mathscr{B}^t$ as $t\to\infty$ and the integrability of (7) ensure the existence of $\lim_{t\to\infty}\mathscr{B}^t=\mathscr{B}^\infty$, and imply

that the dynamical system reaches a statistically steady state. To obtain the evolution equation for $\mathcal{B}^t$, we differentiate (6) with respect to t to obtain[11]

$$\frac{d}{dt}\mathcal{B}^t = I + \mathcal{A}^\dagger \mathcal{B}^t + \mathcal{B}^t \mathcal{A}, \tag{9}$$

with I the identity matrix. The evolution equation is solved with the initial condition $\mathcal{B}^0 = 0$, as can be seen immediately from (6). Taking the $t \to \infty$ limit of (9), we obtain that $\mathcal{B}^\infty$ satisfies the equation

$$\mathcal{A}^\dagger \mathcal{B}^\infty + \mathcal{B}^\infty \mathcal{A} = -I, \tag{10}$$

which was first derived by Lyapunov in another context. This Lyapunov equation can be solved by standard methods.[11] Determination of $\mathcal{B}^\infty$ gives, using (9), a compact form for the time development of $\mathcal{B}^t$:

$$\mathcal{B}^t = \mathcal{B}^\infty - e^{\mathcal{A}^\dagger t} \mathcal{B}^\infty e^{\mathcal{A} t}. \tag{11}$$

Note that when $\mathcal{A}$ is not asymptotically stable $\mathcal{B}^\infty$ diverges, according to the linear dynamics, but that the time development of variance can still be obtained by the direct numerical integration of (9).

The statistically steady-state variance maintained by stochastic forcing follows from (5):

$$\langle E^\infty \rangle = \mathrm{Trace}(\mathcal{F}^\dagger \mathcal{B}^\infty \mathcal{F}) = \mathrm{Trace}(\mathcal{F}\mathcal{F}^\dagger \mathcal{B}^\infty). \tag{12}$$

With a unitary set of forcing functions such that $\mathcal{F}\mathcal{F}^\dagger = I$, the expression for the energy density simplifies to $\langle E^\infty \rangle = \mathrm{Trace}(\mathcal{B}^\infty)$ and the variance is independent of the specific forcing distribution, i.e., any full rank unitary forcing distribution will lead to the same variance.

It is also useful to determine the ensemble average correlation matrix of the response $\mathcal{C}^t_{ij} = \langle x_i(t) x_j^*(t) \rangle$. Following the same steps as in (5) the correlation matrix can be reduced to

$$\begin{aligned}
\mathcal{C}^t_{ij} &= \langle x_i(t) x_j^*(t) \rangle \\
&= \left\langle \int_0^t ds \int_0^t ds' \, \mathcal{G}_{ib}(t-s) \mathcal{F}_{bc} \xi_c(s) \right. \\
&\quad \left. \times \mathcal{G}^*_{je}(t-s') \mathcal{F}^*_{eg} \xi^*_g(s') \right\rangle \\
&= \int_0^t ds \, \mathcal{G}_{ib}(t-s) \mathcal{F}_{bc} \mathcal{F}^*_{ec} \mathcal{G}^*_{je}(t-s),
\end{aligned} \tag{13}$$

or in matrix form,

$$\mathcal{C}^t = \int_0^t \mathcal{G}(t-s) \mathcal{H} \mathcal{G}^\dagger(t-s) ds, \tag{14}$$

with $\mathcal{H} \equiv \mathcal{F}\mathcal{F}^\dagger$. The correlation matrix depends on the dynamical operator $\mathcal{A}$, and the forcing distribution $\mathcal{F}$, unlike $\mathcal{B}^t$, which depends only on the dynamical operator.

We can proceed as previously to determine the evolution equation of $\mathcal{C}^t$. From (14), $\mathcal{C}^0 = 0$ and $\lim_{t\to\infty} \mathcal{C}^t = \mathcal{C}^\infty$ exists when $\mathcal{A}$ is asymptotically stable. Time differentiation of (14) gives the equation governing the temporal evolution of $\mathcal{C}^t$,

$$\frac{d}{dt}\mathcal{C}^t = \mathcal{H} + \mathcal{A}\mathcal{C}^t + \mathcal{C}^t \mathcal{A}^\dagger, \tag{15}$$

with solution

$$\mathcal{C}^t = \mathcal{C}^\infty - e^{\mathcal{A} t} \mathcal{C}^\infty e^{\mathcal{A}^\dagger t}, \tag{16}$$

where the asymptotic stationary correlation matrix, $\mathcal{C}^\infty$, is determined from the solution of the Lyapunov equation:

$$\mathcal{A}\mathcal{C}^\infty + \mathcal{C}^\infty \mathcal{A}^\dagger = -\mathcal{H}. \tag{17}$$

The variance maintained by the stochastic forcing is then $\langle E^\infty \rangle = \mathrm{Trace}(\mathcal{C}^\infty)$. As expected, this value of variance can be shown to be the same as that derived earlier in (12).

Consider now the case of full rank unitary forcing for which $\mathcal{H} = I$. When $\mathcal{A}$ is normal Lyapunov equations (10) and (17) give identical solutions, as can be seen from (6) and (14), but this is not the case when $\mathcal{A}$ is non-normal. The significance of this distinction will be discussed below.

Finally, it is of interest to determine the energy input by the stochastic forcing. This follows from the energy equation in which the energy input appears as

$$\dot{E}_{\mathrm{in}} = \langle x_i^* \mathcal{F}_{ij} \xi_j \rangle + \langle x_i \mathcal{F}^*_{ij} \xi^*_j \rangle. \tag{18}$$

If $\mathcal{F}$ has rank N_f and is assumed unitary in the space spanned by its range, then $\mathrm{Trace}(\mathcal{F}^\dagger \mathcal{F}) = N_f$, and, using (3) and (4), we can reduce (18) to

$$\dot{E}_{\mathrm{in}} = \dot{\epsilon}\, \mathrm{Trace}(\mathcal{F}^\dagger \mathcal{F}) = \dot{\epsilon} N_f, \tag{19}$$

in which $\dot{\epsilon}$ is interpreted as the energy input per forcing function (column of $\mathcal{F}$).

III. THE KARHUNEN–LOEVE DECOMPOSITION FOR NON-NORMAL DYNAMICAL SYSTEMS

In the previous section we showed that the ensemble average energy density for a full rank unitary forcing distribution (for which $\mathcal{H} \equiv \mathcal{F}\mathcal{F}^\dagger = I$) can be derived, either from $\mathcal{B}^t = \int_0^t e^{\mathcal{A}^\dagger(t-s)} e^{\mathcal{A}(t-s)} ds$, or from the correlation matrix $\mathcal{C}^t = \int_0^t e^{\mathcal{A}(t-s)} e^{\mathcal{A}^\dagger(t-s)} ds$. Both $\mathcal{B}^t$ and $\mathcal{C}^t$ are, by construction, positive definite Hermitian forms with positive real eigenvalues associated with mutually orthogonal eigenvalues. Each eigenvalue equals the variance accounted for by the pattern of its corresponding eigenvector, and the pattern that corresponds to the largest eigenvalue contributes most to the variance. The decomposition of the correlation matrix into its orthogonal components is called the Karhunen–Loeve decomposition[12] (referred to as K–L in sequel). This decomposition has been widely used in the analysis of synoptic meteorological data[13] and has also been applied in turbulence research.[14]

The K–L decomposition of $\mathcal{C}^\infty$ determines the structures that contribute most to the ensemble average variance of the statistically steady state. These are the primary response structures of the dynamical system. They are determined by solving the eigenvalue problem:

$$\mathcal{C}^\infty u^{(i)} = \lambda^{(i)} u^{(i)}, \tag{20}$$

in which the variance accounted by the structure $u^{(i)}$ is given by $\lambda^{(i)}$.

Eigenanalysis of $\mathscr{B}^\infty$, on the other hand, allows ordering of the forcing distributions according to their contribution to the variance of the statistically steady state. This follows from (5) and the observation that the eigenvalues of $\mathscr{B}^\infty$, determined from

$$\mathscr{B}^\infty f^{(i)}=\mu^{(i)} f^{(i)}, \tag{21}$$

are also the stationary values of the Rayleigh–Ritz quotient:

$$I[f]=\frac{f'\mathscr{B}^\infty f}{f'f}. \tag{22}$$

The forcings, $f^{(i)}$, obtained from solution of the eigenvalue problem (21) can be ordered according to their relative contribution, $\mu^{(i)}$, to the stochastically maintained variance. In the sequel we will contrast these ordered forcings determined from (21) with the responses ordered according to their contribution to the induced variance determined from (20).

We have determined two sets of orthogonal functions: using (21) we ordered the forcing functions according to their contribution to producing the variance, and using (20) we ordered the response functions according to the fraction of the variance accounted for by each. If the dynamical operator $\mathscr{A}$ is normal, these two sets of orthogonal functions reduce to the eigenfunctions of $\mathscr{A}$ and are identical to the normal modes of the system. This is easily seen because when $\mathscr{A}$ is normal $\mathscr{A}$, $\mathscr{B}^t$, and $\mathscr{C}^t$ commute, and therefore they are simultaneously diagonalized by the same eigenvectors. Consequently, for a normal dynamical operator the K–L patterns have special dynamical significance: they correspond to the normal modes of the dynamical system and also to the forcings that excite the normal modes, and produce the independent modal contributions to the variance. This is not true when $\mathscr{A}$ is non-normal, as is usually the case for fluid dynamical applications. North[15] realized that when the operator $\mathscr{A}$ is non-normal the K–L decomposition of the correlation matrix does not identify the normal modes of $\mathscr{A}$. Identification of the forcings that account for the variance of the statistical steady state for non-normal dynamical systems is an important theoretical question. We have shown that these forcings can be obtained by solving the back Lyapunov equation (10), and we call this the back K–L decomposition. In turn, the response of the dynamical system is obtained by solving the forward Lyapunov equation (17), and we simply call this the K–L decomposition.

Retaining the subspace spanned by the dominant forcing functions found from the back K–L decomposition is at least as important in dynamical investigations of the system, as is retaining the subspace spanned by the dominant response functions found from the K–L decomposition. Restricting representation of the flow dynamics to a subspace spanned by a restricted set of eigenfunctions of the K–L decomposition has been suggested.[14] The above considerations show this to be too restrictive, in general, because it is unlikely in a highly non-normal system that the forcing functions would also be effectively spanned by such a restricted representation.

IV. STOCHASTIC FORCING OF CHANNEL FLOWS

A. Formulation

The nondimensional linearized Navier–Stokes equations governing evolution of disturbances in steady mean flow with the streamwise (x) velocity varying only in the cross-stream direction are

$$\left(\frac{\partial}{\partial t}+U\frac{\partial}{\partial x}\right)\Delta v-U_{yy}\frac{\partial}{\partial x}v=\frac{1}{R}\Delta\Delta v, \tag{23a}$$

$$\left(\frac{\partial}{\partial t}+U\frac{\partial}{\partial x}\right)\omega=\frac{1}{R}\Delta\omega-U_y\frac{\partial}{\partial z}v, \tag{23b}$$

where $U(y)$ is the mean streamwise velocity component, v is the cross-stream perturbation velocity, $\omega\equiv(\partial/\partial z)u-(\partial/\partial x)w$, the cross-stream component of perturbation vorticity (z denotes the spanwise direction), and $\Delta\equiv\partial^2/\partial x^2+\partial^2/\partial y^2+\partial^2/\partial z^2$ is the Laplacian operator. Velocity has been nondimensionalized by U_0, the maximum velocity in the channel; length has been nondimensionalized by L, the half-width of the channel. The Reynolds number is defined as $R\equiv U_0L/\nu$, where ν is the kinematic viscosity. We impose no slip boundary conditions at $y=\pm1$ which are equivalent to $v=(\partial/\partial y)v=\omega=0$ at $y=\pm1$. Couette flow has mean flow $U=y$, and Poiseuille flow has $U=1-y^2$.

Consider a single Fourier component:

$$v=\hat{v}\exp(ikx+ilz), \tag{24a}$$

$$\omega=\hat{\omega}\exp(ikz+ilz), \tag{24b}$$

physical variables being identified with the real part of these complex forms. The field equations can be written in the compact form[7]

$$\frac{\partial}{\partial t}\begin{bmatrix}\hat{v}\\ \hat{\omega}\end{bmatrix}=\begin{bmatrix}\mathscr{L} & 0\\ \mathscr{C} & \mathscr{S}\end{bmatrix}\begin{bmatrix}\hat{v}\\ \hat{\omega}\end{bmatrix}, \tag{25}$$

in which the Orr–Sommerfeld operator $\mathscr{L}$, the Squire operator $\mathscr{S}$, and the coupling operator $\mathscr{C}$ are defined as

$$\mathscr{L}=\Delta^{-1}(-ikU\Delta+ikU_{yy}+\Delta\Delta/R), \tag{26a}$$

$$\mathscr{S}=-ikU+\Delta/R, \tag{26b}$$

$$\mathscr{C}=-ilU_y, \tag{26c}$$

with $K^2=k^2+l^2$ and $\Delta=d^2/dy^2-K^2$.

We define the perturbation energy density, in the usual manner, as

$$E(k,l)=\frac{kl}{16\pi^2}\int_{-1}^{1}dy\int_{0.}^{2\pi/k}dx\int_{0}^{2\pi/l}dz(u^2+v^2+w^2), \tag{27a}$$

$$=\frac{1}{8}\int_{-1}^{1}dy\left(\hat{v}^*\hat{v}+\frac{1}{K^2}\frac{d}{dy}\hat{v}^*\frac{d}{dy}\hat{v}+\frac{1}{K^2}\hat{\omega}^*\hat{\omega}\right), \tag{27b}$$

$$=\frac{1}{8K^2}\int_{-1}^{1}dy\,\psi'\mathcal{M}\psi, \tag{27c}$$

with $\psi=[\hat{v}\ \hat{\omega}]$. The energy metric, $\mathcal{M}$, is given by

$$\mathcal{M}=\begin{bmatrix}-\Delta & 0\\ 0 & I\end{bmatrix}, \tag{28}$$

where I is the identity matrix. In deriving (25b), we made use of

$$\hat{u}=-\frac{i}{K^2}\left(l\hat{\omega}-k\frac{d}{dy}\hat{v}\right), \tag{29a}$$

$$\hat{w}=\frac{i}{K^2}\left(k\hat{\omega}+l\frac{d}{dy}\hat{v}\right). \tag{29b}$$

In deriving (27c), we integrated by parts and made use of the boundary conditions.

Consider now the discrete equivalent of (25). The state vector for an N level discretization is

$$\psi=\begin{bmatrix}\hat{v}_1\\ \vdots\\ \hat{v}_i\\ \vdots\\ \hat{v}_N\\ \hat{\omega}_1\\ \vdots\\ \hat{\omega}_i\\ \vdots\\ \hat{\omega}_N\end{bmatrix}, \tag{30}$$

and the initial value problem (25) assumes the discretized form:

$$\frac{d}{dt}\psi=\mathcal{T}\psi, \tag{31}$$

in which the linear dynamical operator, $\mathcal{T}$, is the discretized form of $\begin{bmatrix}\mathcal{L} & 0\\ \mathcal{C} & \mathcal{S}\end{bmatrix}$. By these means the continuous dynamical system (25) is approximated as a finite-dimensional dynamical system. Correspondence between the continuous and discrete dynamical systems is assumed and convergence is tested by doubling the number of discretization levels.

We wish to determine the evolution of the perturbation energy density, $E(k,l)$. It is advantageous to transform the dynamical equation (31) into variables of the generalized velocities $x=\mathcal{M}^{1/2}\psi$, with $\mathcal{M}$ given in (28). The dynamical equation (31) is then associated with the stochastic dynamical system:

$$\frac{d}{dt}x=\mathcal{A}x+\mathcal{F}\xi, \tag{32}$$

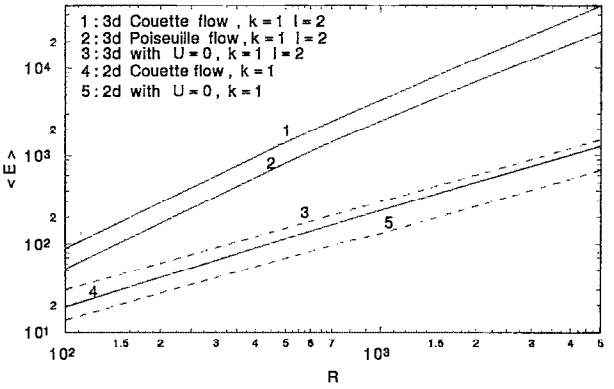

FIG. 1. The ensemble average energy density, $\langle E^{\infty}\rangle$, for various channel flows as a function of Reynolds number, R. Curve 1 is for 3-D perturbations in Couette flow with $k=1$, $l=2$. Curve 2 is for 3-D perturbations in Poiseuille flow with $k=1$, $l=2$. Curve 3 is for 3-D perturbations in a channel with $U=0$ and $k=1$, $l=2$. Curve 4 is for 2-D perturbations in Couette flow and $k=1$. Curve 5 is for 2-D perturbations in a channel with $U=0$ and $k=1$. Curves 3 and 5 are linear in R, while in curves 1 and 2 $\langle E\rangle\approx R^{3/2}$.

where

$$\mathcal{A}=\mathcal{M}^{1/2}\mathcal{T}\mathcal{M}^{-1/2}, \tag{33}$$

ξ is a random Gaussian white noise process, and $\mathcal{F}$ is a forcing distribution initially assumed to provide unit energy density driving to each of the N functions f^i that form the columns of $\mathcal{F}$. In the energy metric the maintained variance corresponds to the ensemble average energy density, $\langle E^{\infty}\rangle=\lim_{t\to\infty}\langle x_i^*(t)x_i(t)\rangle$, of the statistical steady state. (Further discussion of the relation of generalized velocity variables to the normality of $\mathcal{A}$ may be found in the Appendix.) Note that the operator $\mathcal{A}$ is stable, i.e., has a spectrum with negative real parts, for all R in the case of the Couette flow, while for the Poiseuille flow $\mathcal{A}$ is stable for $R<5772.22$.[16,17] We will limit our investigation to $R\leqslant 5000$, so that it may be anticipated that both the Couette and the Poiseuille flow will reach a statistical steady state.

B. The ensemble average energy density

We first determine the variation with Reynolds number of the nondimensional ensemble average energy density. We consider first the Fourier component with $k=1$. The nondimensional ensemble average energy density, $\langle E^{\infty}\rangle$, is a universal function of the Reynolds number R and its dependence on R for a variety of channel flows is shown in Fig. 1. These examples include the 2-D perturbation case with $l=0$ and no flow, i.e., $U=0$, (curve 5), and the 3-D perturbation case with $l=2$ and no flow (curve 3). When there is no flow the associated dynamical system is normal. Note that in both cases with no flow $\langle E^{\infty}\rangle$ grows linearly with R, as would be expected for a normal dynamical system. The increased variance (nearly double) in the flow with 3-D perturbations (curve 3), as compared to the flow with 2-D perturbations (curve 5) can be attributed to the larger number of forcing modes in the former. The $\langle E^{\infty}\rangle$ maintained by 2-D perturbations in

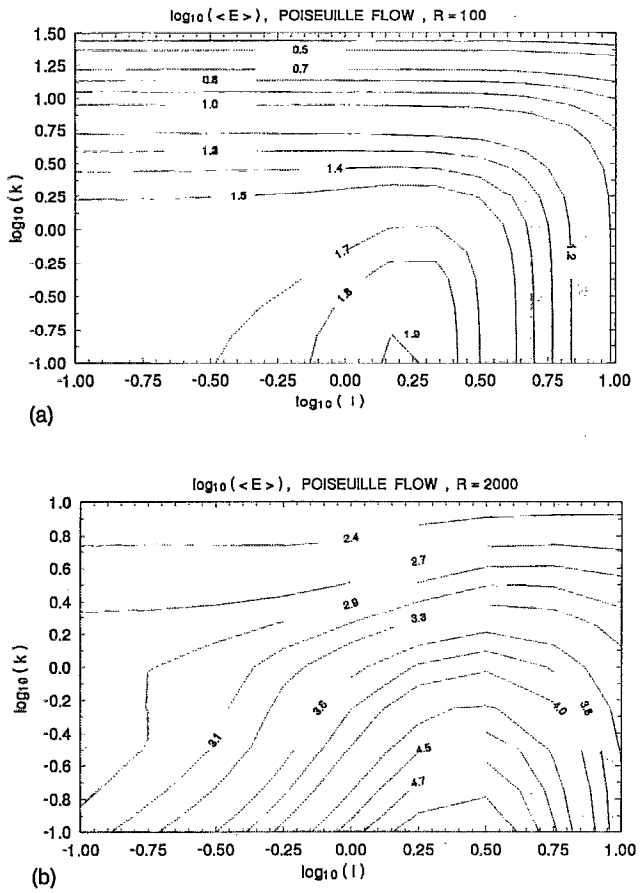

FIG. 2. The ensemble average energy density for 3-D perturbations in Poiseuille flow as a function of k, l, with (a) $R=100$, and (b) $R=2000$.

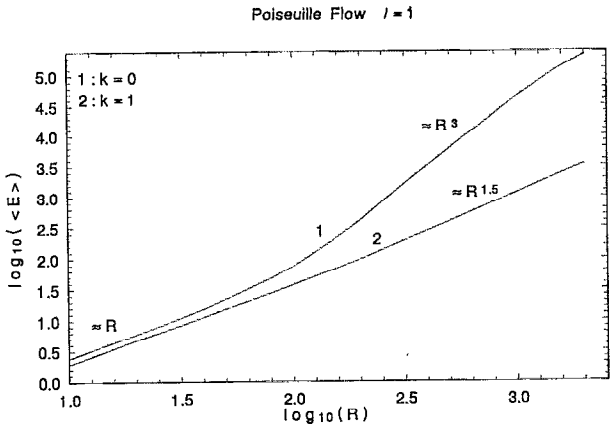

FIG. 3. Variation of ensemble average energy as a function of Reynolds number, R, for 3-D perturbations in plane Poiseuille flow. Both cases are for spanwise wave number $l=1$. Curve 1 is for streamwise wave number $k=0$, and curve 2 for $k=1$.

Couette flow as a function of R is shown in curve 4, from which it is apparent that the non-normality of the operator leads to increased variance compared to that found in the normal system with no flow (curves 3 and 5).

The sustained variance when all 3-D perturbations are allowed is shown as a function of R for the Couette and the Poiseuille flow in Fig. 1, curves (1) and (2), respectively. Note the remarkable increase of variance with Reynolds number ($\langle E^{\infty}\rangle \approx R^{3/2}$). The same dependence on the Reynolds number is found to hold for other choices of k, l, given only that k is not so small as to correspond closely to a streamwise roll.

The total variance for the Poiseuille flow is shown as a function of k and l for $R=100$, and $R=2000$ in Figs. 2(a) and 2(b), respectively. Note that the maximum variance shown occurs on the axis of minimum k. The actual maximum occurs for $k=0$, corresponding to an infinitely extended streamwise roll. The maximum contribution to the variance coincides with the roll axis both because of the growth and the persistence of the roll solutions. While the variance increases sharply near the roll axis ($k=0$), this increase is concentrated in a small area of k,l space. Also, note from Fig. 2 that the (k,l) area that contributes to the total variance increases with R.

The ensemble average energy density sustained by the streamwise roll ($k=0$, $l=1$) is shown as a function of R in Fig. 3. For comparison, the oblique wave with $k=1$ is also shown. The calculation was performed for Poiseuille flow, but similar results hold for the Couette and other stable shear flows examined.[18] For small R the dynamical operator $\mathscr{A}$ [cf. (33)] is dominated by the (normal) diffusion operator, leading to a linear dependence of the variance on R, as is the case for all normal systems for which the sustained variance is inversely proportional to the dissipation. For higher R the variance of the streamwise components grows approximately as R^3. This is due to $O(R^2)$ transient energy growth[7,19] over the time $O(R)$ during which input energy accumulates before it dissipates.

While special initial conditions have been shown to yield robust transient growth,[7–10,19] it does not necessarily follow that arbitrary random initial conditions lead to ensemble average energy growth. We have shown that in the mean the growth of favorably configured perturbations offsets the decay of unfavorably configured perturbations, leading to robust growth of the maintained variance as the Reynolds number increases.

We turn now to the dependence of the maintained dimensional ensemble average energy density [$\langle \widetilde{E}^{\infty}\rangle$ (units J m^{-2})] on the parameters of the flow: the mean shear, U_0/L, and the kinematic viscosity, ν. The nondimensional ensemble average energy density for $\dot{\epsilon}=1$ is $\langle E^{\infty}\rangle = \mathrm{Trace}(\mathscr{C}^{\infty}) \equiv f(R)$, a universal function of the Reynolds number, R. We assume that the dimensional energy input over the channel is prescribed to be $\dot{E}_{\mathrm{in}}$ (units W m^{-2}). Because of the linear relationship between the response and the energy input,

$$\langle \widetilde{E}^{\infty}\rangle = \rho U_0^2 L \dot{\epsilon} f(R), \tag{34}$$

where ρ is the constant density of the fluid. From (19) we relate $\dot{\epsilon}$, the nondimensional energy input per forcing function, to the total energy input:

$$\dot{E}_{\mathrm{in}} = \rho U_0^3 \dot{\epsilon} N_f, \tag{35}$$

where N_f is the number of equally excited forcing functions. Thus we obtain

$$\langle \widetilde{E^{\infty}} \rangle = \frac{L}{U_0} \dot{E}_{\text{in}} \frac{f(R)}{N_f}. \tag{36}$$

For Fourier components off the roll axis (i.e., $k \neq 0$) $f(R) \approx R^{3/2}$. Consequently, for flows with the same U_0 and the same geometry the maintained dimensional variance as a function of ν will behave as

$$\langle \widetilde{E^{\infty}_{k\neq 0}} \rangle = C\dot{E}_{\text{in}} \frac{1}{\nu^{3/2}}, \tag{37}$$

where C is a dimensional constant. For flows with the same kinematic viscosity but different mean shears $s \equiv U_0/L$, the dependence of the maintained variance on shear is

$$\langle \widetilde{E^{\infty}_{k\neq 0}} \rangle = C\dot{E}_{\text{in}} s^{1/2}. \tag{38}$$

For streamwise rolls (i.e., $k=0$), $f(R) \approx R^3$. For flows with the same U_0 and the same geometry, the maintained dimensional variance as a function of ν will then be

$$\langle \widetilde{E^{\infty}_{k=0}} \rangle = C\dot{E}_{\text{in}} \frac{1}{\nu^{3}}, \tag{39}$$

where C is a dimensional constant. For flows with the same kinematic viscosity but different mean shears, $s \equiv U_0/L$, the dependence of the maintained variance on shear for the streamwise rolls is

$$\langle \widetilde{E^{\infty}_{k=0}} \rangle = C\dot{E}_{\text{in}} s^{2}. \tag{40}$$

Comparison of (38) and (40) suggests that for a given fluid increasing shear favors the emergence of streamwise rolls.

C. The K–L and back K–L decomposition for the Couette and Poiseuille flow

The contribution of the forcing functions, $\mu^{(i)}$, to the ensemble average energy as determined from (21), are shown in Fig. 4(a). Similarly the contribution of the response functions, $\lambda^{(i)}$, to the total variance, determined from (20), are shown in Fig. 4(b). Note that only a few of the response functions are required to account for most of the variance. This is a property of the K–L decomposition: it provides the most parsimonious orthogonal basis functions and typically most of the variance arises from a small subset of leading modes. For example, in the Poiseuille flow with $k=1$ and $l=2$ at $R=100$, the first four modes account for 75% of the variance, and the first 85 modes account for 99% of the variance. For $R=1000$ the first four modes account for 92% of the variance. At $R=5000$ the first four modes account for 82% of the variance, and 99% of the variance, is accounted for by the first 30 modes. It is important to note that these results do not depend on the discretization, as long as the main contribution to the variance has been resolved.

For a specific Fourier component the contribution of each mode to the variance decays rapidly with mode number rendering the total variance convergent as the number of modes increases, as can be seen, for example, from Fig. 4. If we were to excite all modes, each with unit energy, we would need divergent total energy forcing as our resolution

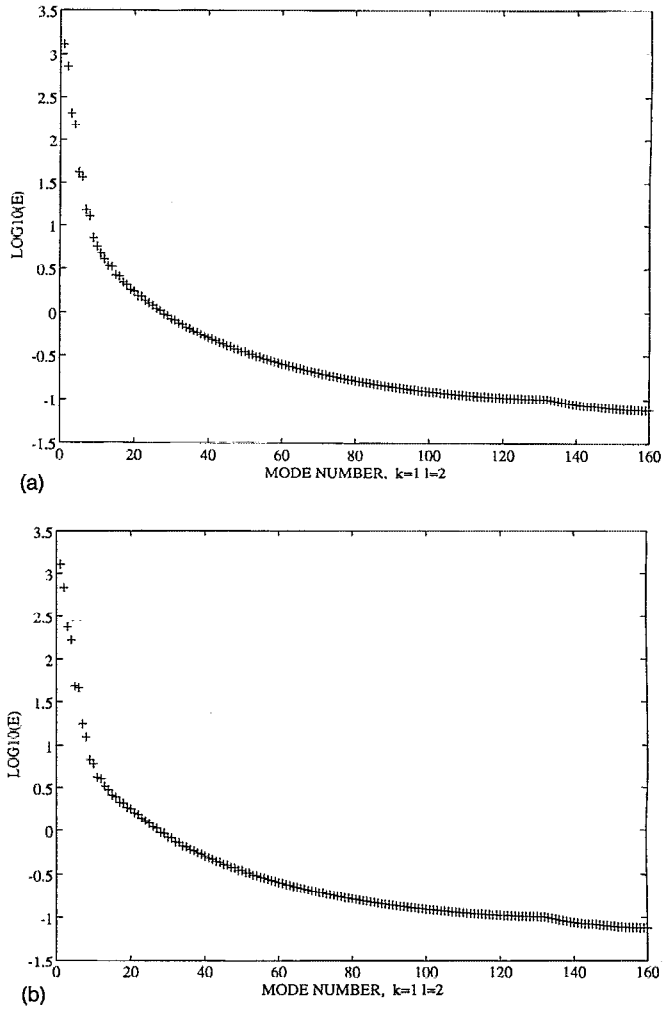

FIG. 4. Contribution of forcing and response functions to total variance. The case shown is Poiseuille flow with $k=1$, $l=2$, and $R=1000$. The maintained total variance is 2553 for unit forcing of each degree of freedom. (a) Variance resulting from the ordered forcing functions. (b) Variance resulting from the ordered response functions.

increased. This situation is common to the statistical mechanics of classical systems. While ensemble average energy for a specific Fourier component converges as the number of modes increases, Fig. 2 indicates that a low pass truncation is necessary to assure finiteness of the total power input under the assumption of white noise forcing.

Figures 5(a) and 5(b) show the single forcing distribution that produces the most variance in Couette flow at $R=1000$. Note that the structure is similar to that of an optimal excitation of the flow.[7] The response pattern, the first K–L pattern, for Couette flow at $R=1000$ is shown in Figs. 5(c) and 5(d). Note the difference between the forcing and response structures remarked on previously. This is a characteristic property of non-normal dynamical operators. The corresponding structures for Poiseuille flow are shown in Figs. 6(a)–6(d). Note that the dominant response of both the Poiseuille and Couette flow exhibits the characteristic streak structure.

V. CONCLUSIONS

Observations of transition from laminar to turbulent flow have consistently shown, since the experiments of

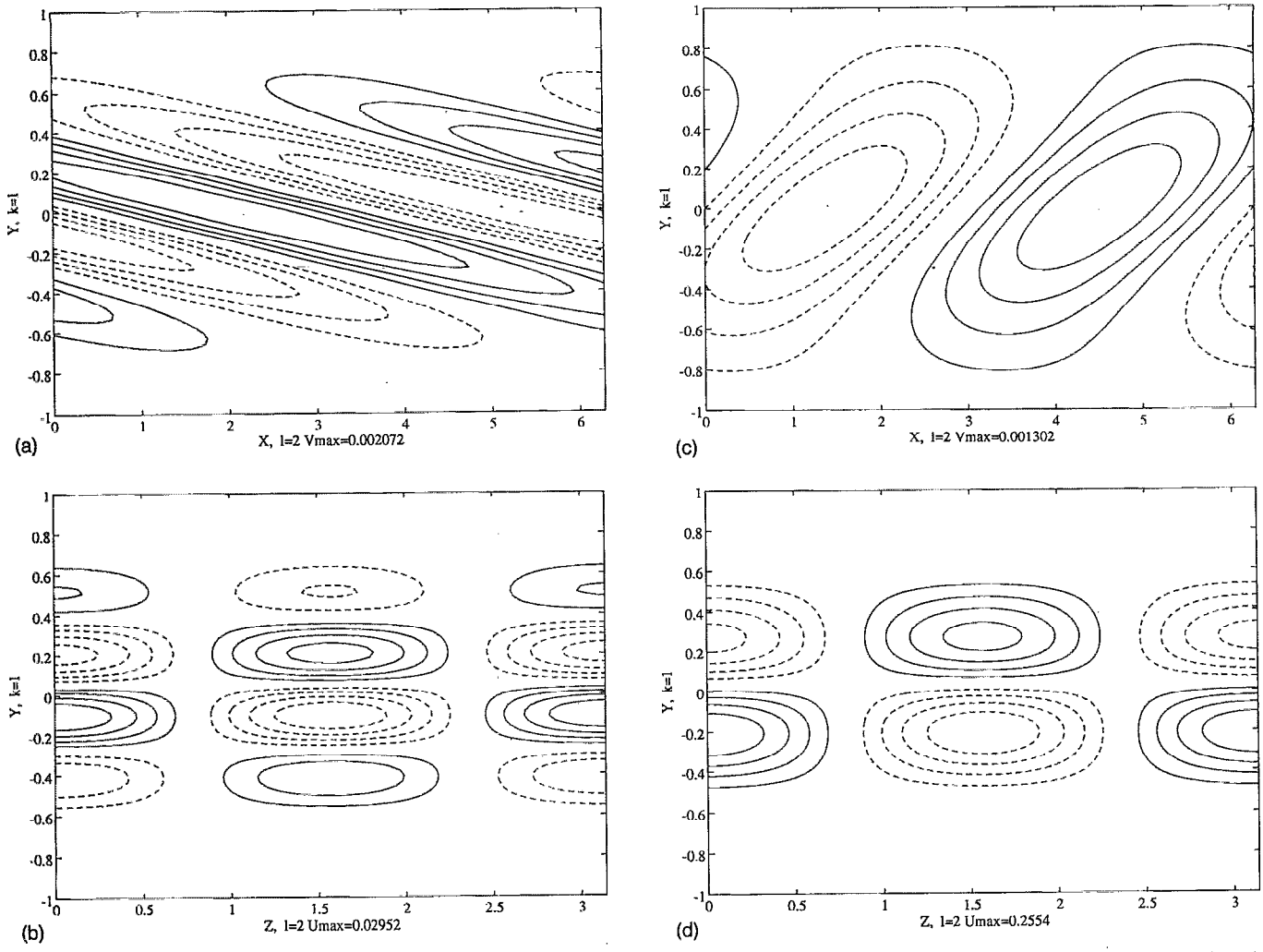

FIG. 5. Structure of the principal forcing and response functions for Couette flow with $k=1$, $l=2$, and $R=1000$. The maintained total variance is 4244 for unit forcing of each degree of freedom. (a) The principal forcing function cross-stream velocity, v, in the x-y plane. (b) The principal forcing function streamwise velocity, u, in the y-z plane. The principal forcing function contributes 1855 units to the total variance. (c) The principal response function cross-stream velocity, v, in the x-y plane. (d) The principal response function streamwise velocity, u, in the y-z plane. The principal response function contributes 1749 units to the total variance.

Reynolds,[20] that transition is highly sensitive to background disturbances. A reason for this sensitivity arises from the existence of a subset of optimal perturbations that produce high levels of transient growth, even though these canonical problems typically are asymptotically stable at the Reynolds numbers for which transition is found to occur.[7–10,19] Unless the background disturbance field is contrived to have a null projection on these growing disturbances, they can amplify sufficiently to instigate transition when forcing typical of ambient background noise in experiments is imposed.

While the theory leading to identification of optimal excitations addresses transient growth as an initial value problem, we have shown in this work that a continuous stochastic excitation of viscous shear flow produces high levels of variance if the Reynolds number of the flow is sufficiently large. This variance arises primarily from excitation of a restricted subset of favorably configured forcing functions, distinct from the optimal perturbations, which can be found as the solutions of a Lyapunov equation. In a similar manner, the response functions that form the primary structures of the maintained variance can be identified with solutions of a related Lyapunov equation. The primary forcing functions determine a low-dimensional subspace that must be spanned by a basis for the stochastic dynamics, while the primary response functions similarly determine a subspace that must also be spanned by the dynamical basis. The distinction between the forcing and response functions is a consequence of the non-normality of the linear dynamical operator, and no such distinction arises in unsheared flow, unsheared convection, or other dynamical systems characterized by normal operators.

Only a slight extension of this mechanism for maintenance of variance under stochastic forcing is required to at least conceptually rationalize the maintenance of the fully turbulent state. The elements of this construction comprise the already demonstrated great amplification of a subset of perturbations, together with a mechanism to replenish the growing subspace, as the members are depleted through their transient evolution, so as in this way to produce a

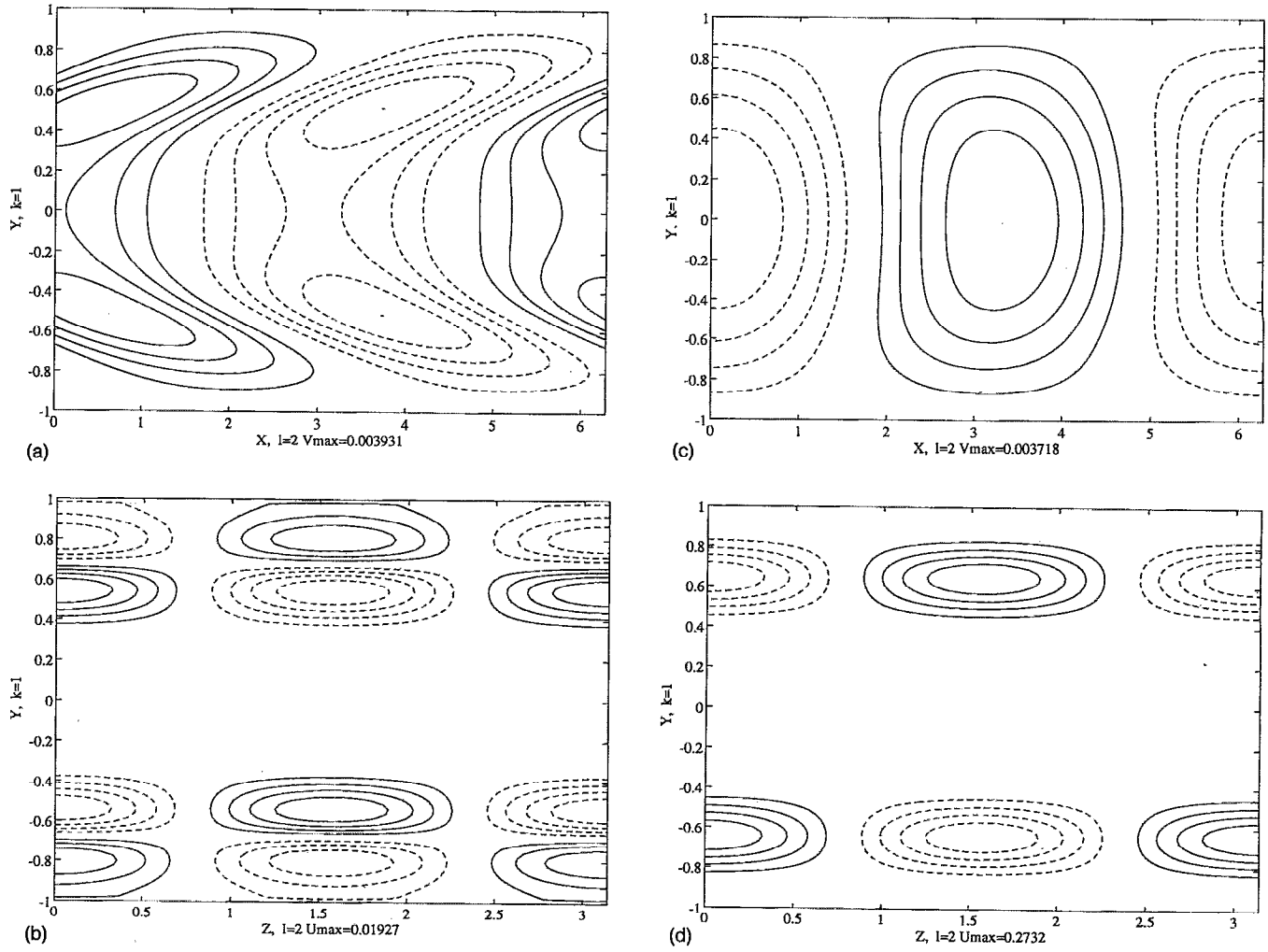

FIG. 6. Structure of the principal forcing and response functions for Poiseuille flow with $k=1$, $l=2$, and $R=1000$. The maintained total variance is 2518 for unit forcing of each degree of freedom. (a) The principal forcing function cross-stream velocity, v, in the x-y plane. (b) The principal forcing function streamwise velocity, u, in the y-z plane. The principal forcing function contributes 1305 units to the total variance. (c) The principal response function cross-stream velocity, v, in the x-y plane. (d) The principal response function streamwise velocity, u, in the y-z plane. The principal response function contributes 1268 units to the total variance.

statistical mean state. The obvious candidate mechanism to replenish the subset of growing perturbations is the nonlinear interactions of the perturbations that were neglected in the linear dynamics. The requisite scattering of energy back into the growing subspace need not be particularly efficient, given the great amplification of the members of this subspace. We may model this process by observing that the $k^{-5/3}$ spectrum of isotropic turbulence is produced on the time scale of the eddy turnover at a particular scale. The nonlinear interactions also tend to disrupt the coherence of the growing disturbances on the same eddy turnover time scale.[8,21] It can be expected then that the level of variance will rise until these competing processes of replenishment and disruption obtained a statistical balance, with a variance level such as to produce an eddy turnover time at the dynamically dominant scales of a small multiple of the shear time scale.

While the task of explicitly modeling maintenance of the fully turbulent state is beyond the scope of the present study, the great amplification of variance demonstrated in this work shows the rich dynamics of asymptotically stable shear flows.

ACKNOWLEDGMENTS

Brian Farrell was supported by National Science Foundation contract No. ATM-92-16813. Petros Ioannou was supported by National Science Foundation contract No. ATM-92-16189. PJI also acknowledges the support of the National Science Foundation through the Woods Hole Oceanographic Institution Geophysical Fluid Dynamics Summer Program.

APPENDIX: THE ORTHOGONAL NORM METRIC

The non-normality of the operator,

$$\mathcal{A}=\mathcal{M}^{1/2}\mathcal{T}\mathcal{M}^{-1/2}, \tag{A1}$$

was shown in Sec. IV to greatly influence the statistics of the dynamical system. It is clear from (A1) that the use of different norms to measure perturbation magnitude alters

the normality of the dynamical system.[15,22] The freedom to choose a norm allows the investigator to concentrate on those aspects of the dynamics that are of greatest interest. This issue has often been neglected, perhaps because all norms are equivalent for white noise excitation of the orthogonal modes of normal dynamical systems. We have chosen $\mathcal{M}$ to correspond to energy density in which case $\mathcal{A}$ is non-normal for the shear flows examined. Because of the importance of the non-normality of $\mathcal{A}$ in determining the associated stochastic dynamics, it is of interest to determine the most general $\mathcal{M}$ that renders $\mathcal{A}$ a normal operator.

If $\mathcal{A}$ is normal then $\mathcal{A}\mathcal{A}^\dagger = \mathcal{A}^\dagger\mathcal{A}$, which is equivalent to

$$\mathcal{T}\mathcal{M}^{-1}\mathcal{T}^\dagger\mathcal{M} = \mathcal{M}^{-1}\mathcal{T}^\dagger\mathcal{M}\mathcal{T}. \tag{A2}$$

Hence $\mathcal{T}$ and $\mathcal{M}^{-1}\mathcal{T}^\dagger\mathcal{M}$ commute and have the same eigenvectors. If we denote by Φ the matrix consisting of the eigenvectors of $\mathcal{T}$ arranged in columns, then

$$\mathcal{M}^{-1}\mathcal{T}^\dagger\mathcal{M}\Phi = \Phi\mathcal{S}, \tag{A3}$$

where $\mathcal{S}$ is a diagonal matrix. Hence

$$\mathcal{T}^\dagger\mathcal{M}\Phi = \mathcal{M}\Phi\mathcal{S}. \tag{A4}$$

Therefore $\mathcal{M}\ \Phi$ is the eigenvector matrix of $\mathcal{T}^\dagger$, which, because Φ is the eigenvector matrix of $\mathcal{T}$, has the eigenvector matrix $\Phi^{\dagger-1}$. Hence

$$\mathcal{M}\Phi = \Phi^{\dagger-1}\mathcal{D}^{-1}, \tag{A5}$$

where $\mathcal{D}^{-1}$ is any positive definite diagonal matrix. Thus, we have shown that the most general metric that renders $\mathcal{A}$ normal is

$$\mathcal{M} = (\Phi\mathcal{D}\Phi^\dagger)^{-1}. \tag{A6}$$

The related norm is the measure of perturbation magnitude consisting of a weighted sum of the squared amplitudes of the modes that make up the perturbation. We have shown that this is the only norm in which the modes are orthogonal. Despite the apparent simplicity gained by the fact that the dynamical system is normal in these generalized coordinates, the sum of squared amplitudes of the modes making up a disturbance has no obvious physical significance such as attaches to perturbation energy or enstrophy.

[1] V. W. Ekman, "On the the change from steady to turbulent flow of liquids," Ark. Mat. Astron. Fys. **6**, 12 (1910).

[2] W. Pfenninger, "Boundary layer suction experiments with laminar flow at high Reynolds numbers in the inlet length of a tube by various suction methods," in *Boundary Layer and Flow Control*, edited by G. V. Lachmann (Pergamon, Oxford, 1961), p. 970.

[3] D. D. Joseph, *Stability of Fluid Motions I* (Springer-Verlag, New York, 1976).

[4] R. Kubo, M. Toda, and N. Hashitsume, *Statistical Physics II* (Springer-Verlag, New York, 1983).

[5] W. M'F. Orr, "The stability or instability of the steady motions of a perfect liquid and of a viscous liquid," Proc. R. Irish Acad. Ser. A **27**, 9 (1907).

[6] B. F. Farrell and P. J. Ioannou, "Stochastic forcing of perturbation variance in unbounded shear and deformation flows," J. Atmos. Sci. **50**, 200 (1993).

[7] K. M. Butler and B. F. Farrell, "Three-dimensional optimal perturbations in viscous shear flow," Phys. Fluids A **4**, 1637 (1992).

[8] B. F. Farrell and P. J. Ioannou, "Optimal excitation of three-dimensional perturbations in viscous constant shear flow," Phys. Fluids A **5**, 1390 (1993).

[9] L. H. Gustavsson, "Energy growth of three dimensional disturbances in plane Poiseuille flow," J. Fluid Mech. **98**, 149 (1991).

[10] S. C. Reddy and D. S. Henningson, "Energy growth in viscous channel flows," J. Fluid Mech. **252**, 209 (1993).

[11] S. Lefschetz, *Differential Equations: Geometric Theory* (Dover, New York, 1963).

[12] M. Loeve, *Probability Theory* (Springer-Verlag, New York, 1978), Vol. II.

[13] E. N. Lorenz, "Empirical orthogonal functions and statistical weather prediction," Report 1, Statistical Forecasting Project, Massachusetts Institute of Technology, 1956.

[14] J. L. Lumley, "The structure of inhomogeneous turbulent flows," in *Atmospheric Turbulence and Radio Wave Propagation*, edited by A. M. Yaglom and V. I. Tatarsky (Nauka, Moscow, 1967), p. 166.

[15] G. R. North, "Empirical orthogonal functions and normal modes," J. Atmos. Sci. **41**, 879 (1984).

[16] W. Heisenberg, "Über Stabilität und Turbulenz von Flussingkeitsströmen," Ann. Phys. Lpz. **74**, 577 (1924).

[17] S. A. Orszag, "Accurate solution of the Orr–Sommerfeld stability equation," J. Fluid Mech. **50**, 689 (1971).

[18] B. F. Farrell and P. J. Ioannou, "Perturbation growth in shear flow exhibits universality," Phys. Fluids A **5**, 2298 (1993).

[19] L. N. Trefethen, A. E. Trefethen, S. C. Reddy, and T. A. Driscoll, "Hydrodynamic stability without eigenvalues," Science **261**, 578 (1993).

[20] O. Reynolds, "An experimental investigation of the circumstances which determine whether the motion of water shall be direct or sinuous, and the law of resistance in parallel channels," Philos. Trans. **51**, 935 (1883).

[21] K. B. Butler and B. F. Farrell, "Optimal perturbations and streak spacing in wall bounded shear flow," Phys. Fluids A **5**, 774 (1993).

[22] B. F. Farrell, "Optimal excitation of perturbations in viscous shear flow," Phys. Fluids **31**, 2093 (1988).